J. Vis. Commun. Image R. 25 (2014) 1791–1799

Contents lists available at ScienceDirect

J. Vis. Commun. Image R.

journal homepage: www.elsevier.com/locate/jvci

Short Communication

An improved universal subsampling strategy for compressing mosaic videos with arbitrary RGB color filter arrays in H.264/AVC

Yung-Hsiang Chiu, Kuo-Liang Chung, Chien-Hsiung Lin *

Department of Computer Science and Information Engineering, National Taiwan University of Science and Technology, No. 43, Section 4, Keelung Road, Taipei 10672, Taiwan, ROC

ARTICLE INFO

Article history:
Received 24 April 2014
Accepted 19 July 2014
Available online 27 July 2014

Keywords:
4:2:0 subsampling format
Arbitrary RGB color filter arrays
Compression
H.264/AVC
Mosaic videos
RGB color deviation problem
Subsampling strategy
Y luma component modification

ABSTRACT

This work proposes an improved version of Yang et al.'s universal subsampling strategy for compressing mosaic videos with arbitrary red–green–blue (RGB) color filter arrays in H.264/AVC. For the subsampled images with 4:2:0 format, Yang et al.'s work retains the original Y luma component, but samples the proper *U* and *V* chroma components according to the corresponding mosaic structure for better reconstructing *R* and *B* pixels. However, Yang et al.'s strategy suffers from the RGB color deviations due to the *U* and *V* chroma subsampling, which results in the quality degradation of the reconstructed mosaic videos. We propose a novel modification for the Y luma component instead of only retaining the Y luma component such that the RGB color deviation problem can be resolved. Experimental results demonstrate that the proposed improved universal subsampling strategy delivers better quality of the reconstructed mosaic and full-color videos, when compared with Yang et al.'s one.

1. Introduction

Recently, mobile devices combined with digital cameras have become increasingly ubiquitous in the consumer electronics market. In consideration of cost, these digital cameras integrated in mobile devices are usually equipped with a single charge-coupled device (CCD) or complementary metal oxide semiconductor (CMOS) sensor, the surface of which is covered with a red–green–blue (RGB) color filter array (CFA) as shown in Fig. 1, for each pixel to capture the color information of real-world scenes [17]. Each pixel in the images of the acquired video has only one of three RGB primary color components and hence such a video is referred to as a mosaic video. For mosaic videos, the RGB CFA structure is required for the following video processing, such as demosaicking [18,15,11] and super-resolution [8,12], and can be obtained from the camera manufacturer or the header of the raw CFA video in TIFF-EP format. Ten commonly used types of RGB CFA structures [16] are shown in Fig. 2, of which the Bayer CFA [1] is the most well-known structure.

Compression of mosaic videos is a key component in consumer digital cameras due to the considerations of economical storage and transmission over the Internet. Most existing schemes for compressing mosaic videos concentrate on employing either structure conversion [9,6,7] or demosaicking [4,19] prior to compression for achieving better compression performance. Structure conversion based compression schemes, which convert the CFA structure into three RGB distinct color planes for compression, are often applied to mosaic videos with the Bayer CFA since the Bayer CFA has 2:1:1 (G:B:R) color component composition in each 2×2 subimage, which is similar to the 4:2:2 subsampling format used by the encoder. However, due to the requirement of a specific subsampling format by the encoder and the difficulty of converting irregular CFA structures, the structure conversion based compression schemes cannot be applied directly to mosaic videos with non-Bayer CFA structures.

In contrast, demosaicking based compression schemes are applicable to different types of mosaic videos with the aid of demosaicking techniques designed for one specific CFA structure or universal demosaicking techniques for arbitrary CFA structures. Prior to compression, Chen et al. [4] first demosaicked the mosaic videos with the Bayer CFA by bilinear interpolation to recover the full RGB colors and then adjusted the *U* and *V* chroma subsampling strategy with 4:2:0 format in H.264/AVC [5] to improve the quality of the reconstructed mosaic videos. Yang et al. [19] proposed a universal scheme for compressing mosaic videos with arbitrary CFA structures in H.264/AVC, which basically works, prior to compression, with the universal demosaicking technique slightly modified from [15] first and then the proposed universal *U* and *V* chroma subsampling strategy with 4:2:0 format. Specifically, Yang et al.'s chroma subsampling strategy has the same compression performance as Chen et al.'s one for mosaic videos with the Bayer

* Corresponding author.
E-mail address: d9409301@mail.ntust.edu.tw (C.-H. Lin).

http://dx.doi.org/10.1016/j.jvcir.2014.07.003
1047-3203/

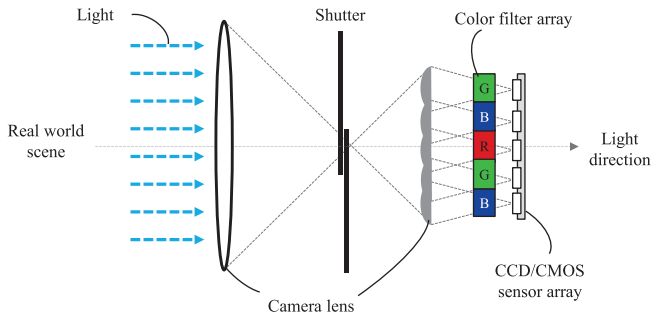

Fig. 1. The camera model with a RGB CFA structure for capturing mosaic videos.

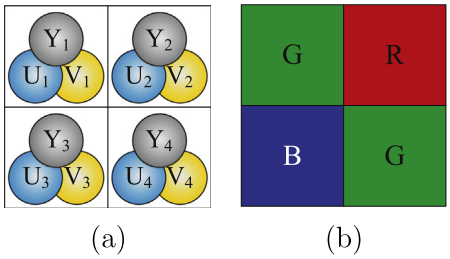

Fig. 3. (a) One 2 × 2 YUV block and (b) its associated mosaic block.

CFA, and has superior compression performance over the traditional one in H.264/AVC for mosaic videos with arbitrary CFA structures.

The advantage of Yang et al.'s chroma subsampling strategy for compressing mosaic videos with arbitrary CFA structures lies in that it selects the proper pixels to sample the shared *U* and *V* components by considering the corresponding CFA structure and the significance of the *U* and *V* components for reconstructing *R* and *B* pixels. Since, when reconstructing the *R* pixels for the reconstructed mosaic video, *V* components are more significant than *U* components, Yang et al.'s strategy determines, when encoding, the shared *V* component associated with a 2 × 2 YUV block by averaging the *V* components corresponding to the *R* pixels in the associated mosaic block. Similarly, the shared *U* component associated with the block, when encoding, is determined as the average of the *U* components corresponding to the *B* pixels in the associated mosaic block. For example, considering the 2 × 2 YUV block and its associated mosaic block shown in Fig. 3, Yang et al.'s strategy determines the shared *U* and *V* components of the current YUV block as U_3 and V_2, respectively.

However, these demosaicking based compression schemes suffer from RGB color deviations due to the *U* and *V* chroma subsampling, which results in quality degradation of the reconstructed mosaic videos. For example, Fig. 4 gives a real 2 × 2 subimage from the *Houses* video with the Bayer CFA to perform Yang et al.'s compression scheme. To illustrate the so-called RGB color deviation problem, after executing each step of Yang et al.'s compression scheme, we perform proper inverse operations on the resultant subimage to obtain the corresponding mosaic color values of the subimage. It can be found that the original mosaic color values of the subimage no longer keep intact after the *U* and *V* chroma subsampling in Step 3, indicating that Yang et al.'s subsampling strategy is actually the reason for incurring the RGB color deviations.

To solve the above RGB color deviation problem which occurs in subsampling, in this work, we propose an improved version of Yang et al.'s universal subsampling strategy for compressing mosaic videos with arbitrary RGB color filter arrays in H.264/AVC. Under the framework of Yang et al.'s universal subsampling strategy, we replace retaining the original Y luma component with adopting a novel modification for the Y luma component such that the RGB color deviation problem can be resolved. The experimental results demonstrate that the proposed improved subsampling strategy can deliver better quality of the reconstructed mosaic videos and the reconstructed full-color videos under the same bitrate, when compared with the state-of-the-art one by Yang et al.

The rest of this work is organized as follows. In Section 2, we present the proposed improved universal subsampling strategy for compressing mosaic videos with arbitrary RGB CFA structures in H.264/AVC. Based on the four test videos with the ten commonly used RGB CFA structures, Section 3 gives the empirical results of

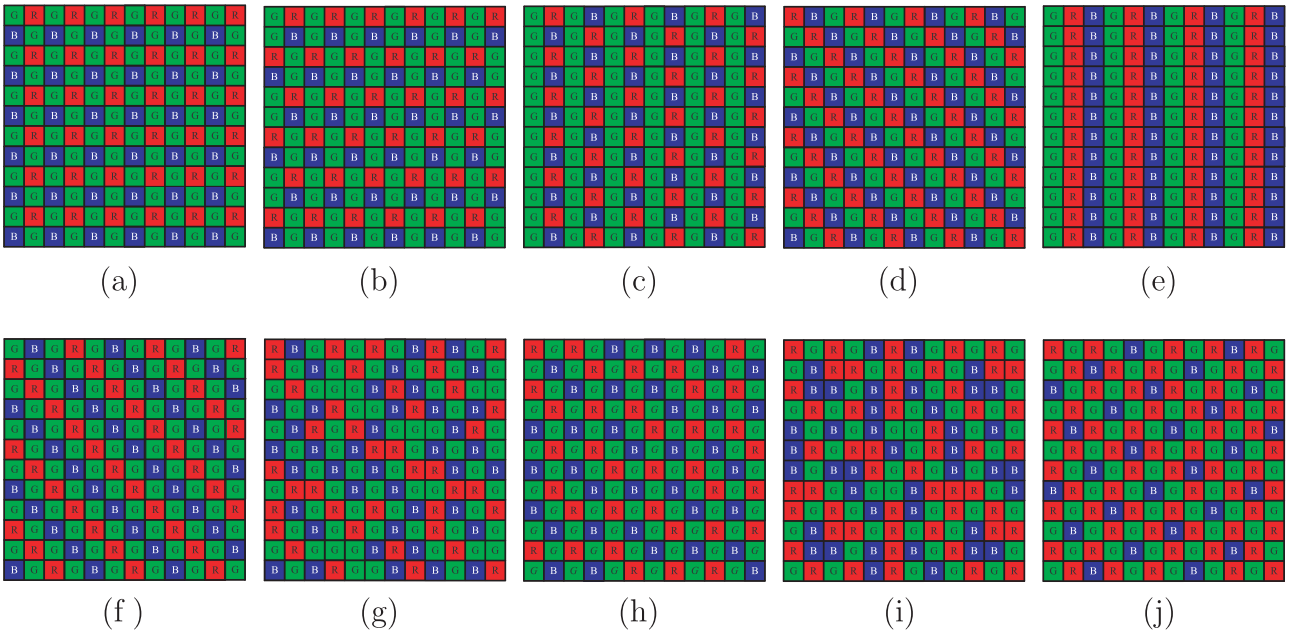

Fig. 2. Ten commonly used RGB CFA structures: (a) Bayer CFA. (b) Lukac and Plataniotis CFA. (c) Yamanaka CFA. (d) Diagonal stripe CFA. (e) Vertical stripe CFA. (f) Modified Bayer CFA. (g) HVS-based CFA. (h) Type I Pseudo-random CFA. (i) Type II Pseudo-random CFA. (j) Type III Pseudo-random CFA.

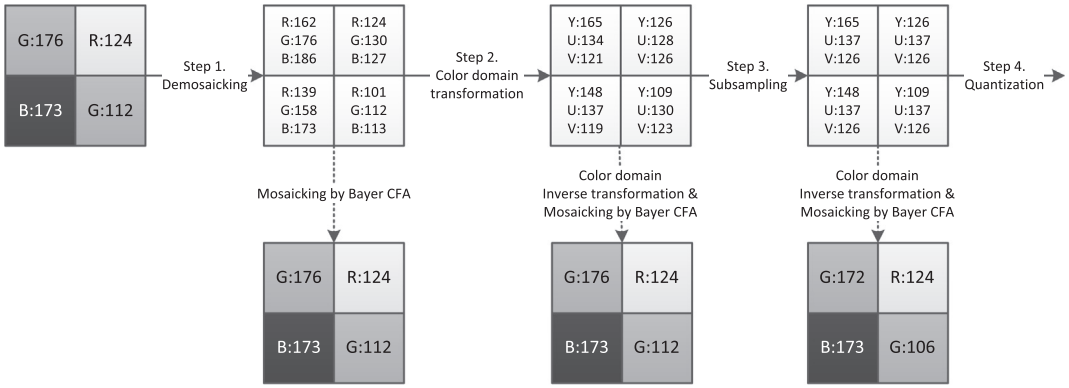

Fig. 4. An example of the RGB color deviations resulting from the U and V chroma subsampling with 4:2:0 format.

the compression performance in terms of the quality of the reconstructed mosaic videos and the reconstructed full-color videos as well as the bitrate requirement. Concluding remarks are given in Section 4.

2. Proposed improved universal subsampling strategy

For a mosaic image I_M in the input mosaic video with an arbitrary RGB CFA structure, let I_{YUV} represent the corresponding YUV image, which is obtained by performing both the universal demosaicking technique modified from [15] and the RGB to YUV color domain transformation defined as

$$\begin{bmatrix} Y \\ U \\ V \end{bmatrix} = \begin{bmatrix} 0.257 & 0.504 & 0.098 \\ -0.148 & -0.291 & 0.439 \\ 0.439 & -0.368 & -0.071 \end{bmatrix} \begin{bmatrix} R \\ G \\ B \end{bmatrix} + \begin{bmatrix} 16 \\ 128 \\ 128 \end{bmatrix} \tag{1}$$

on I_M. To compress I_{YUV} in 4:2:0 format by the H.264/AVC encoder, for each 2×2 block in I_{YUV}, only four Y components, one shared U component, and one shared V component can be stored for compression. Considering a 2×2 block in I_{YUV}, let $F^L_{YUV}(i,j)$ denote the value of component L ($L \in Y,U,V$) of the pixel at position (i,j), i.e., row i and column j, of the block and $F^C_M(i,j)$ denote the value of component C ($C \in R,G,B$) of the pixel at position (i,j) of its co-located 2×2 block in the mosaic image I_M.

Before delivering the proposed RGB color deviation-free subsampling result for the current 2×2 block in I_{YUV}, we first adopt the U and V determination process by Yang et al. to yield the shared U component and V component of the current block

$$U^* = \begin{cases} \frac{1}{|\mathbb{S}^B|} \sum_{(i,j) \in \mathbb{S}^B} F^U_{YUV}(i,j), & \text{if } |\mathbb{S}^B| \neq 0, \\ \frac{1}{4} \sum_{i=1}^{2} \sum_{j=1}^{2} F^U_{YUV}(i,j), & \text{otherwise}, \end{cases} \tag{2}$$

$$V^* = \begin{cases} \frac{1}{|\mathbb{S}^R|} \sum_{(i,j) \in \mathbb{S}^R} F^V_{YUV}(i,j), & \text{if } |\mathbb{S}^R| \neq 0, \\ \frac{1}{4} \sum_{i=1}^{2} \sum_{j=1}^{2} F^V_{YUV}(i,j), & \text{otherwise}, \end{cases} \tag{3}$$

where $\mathbb{S}^B$ denotes the set of positions of the B color pixels in its co-located 2×2 block in I_M and $\mathbb{S}^R$ is defined like $\mathbb{S}^B$ but for the R color pixels.

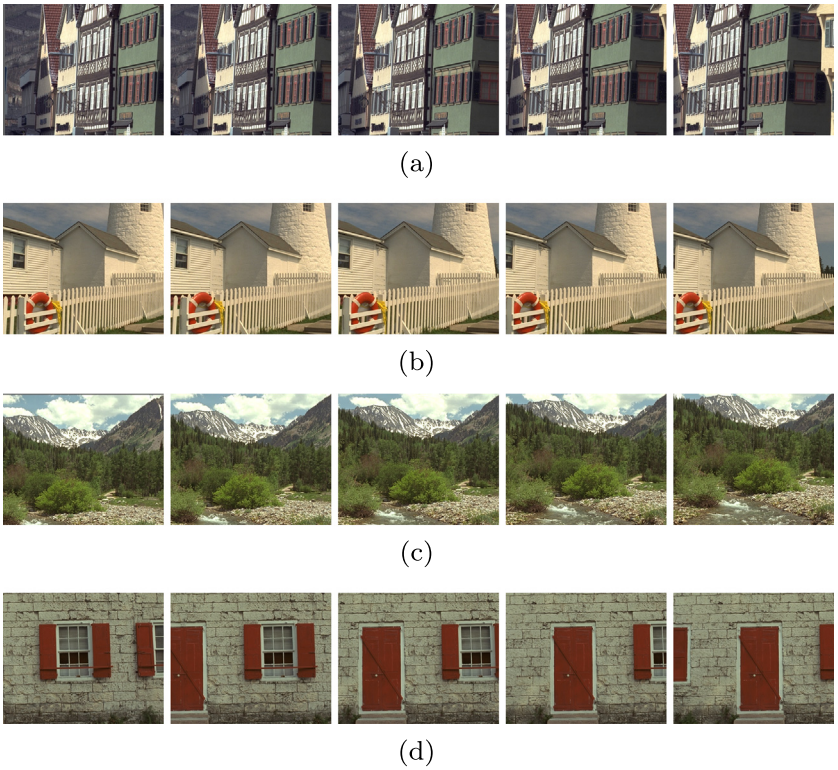

Fig. 5. Four test videos: (a) *Houses*. (b) *Lighthouse*. (c) *Nature*. (d) *Wall*.

After obtaining the shared U and V components (U^*, V^*), we then determine a proper Y component for each pixel of the current block instead of only retaining the original Y component by Yang et al. such that the RGB color deviation problem can be resolved. Suppose that the pixel at position (i,j) of the current block corresponds to a C $(C \in R, G, B)$ color pixel at position (i,j) of the co-located block in I_M. Based on the YUV to RGB color domain transformation

$$\begin{bmatrix} R \\ G \\ B \end{bmatrix} = \begin{bmatrix} 1.164 & 0 & 1.596 \\ 1.164 & -0.391 & -0.813 \\ 1.164 & 2.018 & 0 \end{bmatrix} \begin{bmatrix} Y-16 \\ U-128 \\ V-128 \end{bmatrix}, \tag{4}$$

since the shared U and V components have been determined as U^* and V^*, for the pixel at position (i,j) of the current block, its inverse mosaic color value $\widehat{F}^C_M(i,j)$ and Y component have the following relationship

$$\widehat{F}^C_M(i,j) = \begin{cases} 1.164 \times (Y-16) + 1.596 \times (V^*-128), & \text{if } C = R, \\ 1.164 \times (Y-16) - 0.391 \times (U^*-128) - 0.813 \times (V^*-128) & \text{if } C = G, \\ 1.164 \times (Y-16) + 2.018 \times (U^*-128), & \text{if } C = B. \end{cases} \tag{5}$$

To achieve no RGB color deviation for the pixel at position (i,j), which means that the inverse mosaic color value $\widehat{F}^C_M(i,j)$ needs to be equal to the original mosaic color value $F^C_M(i,j)$, we substitute

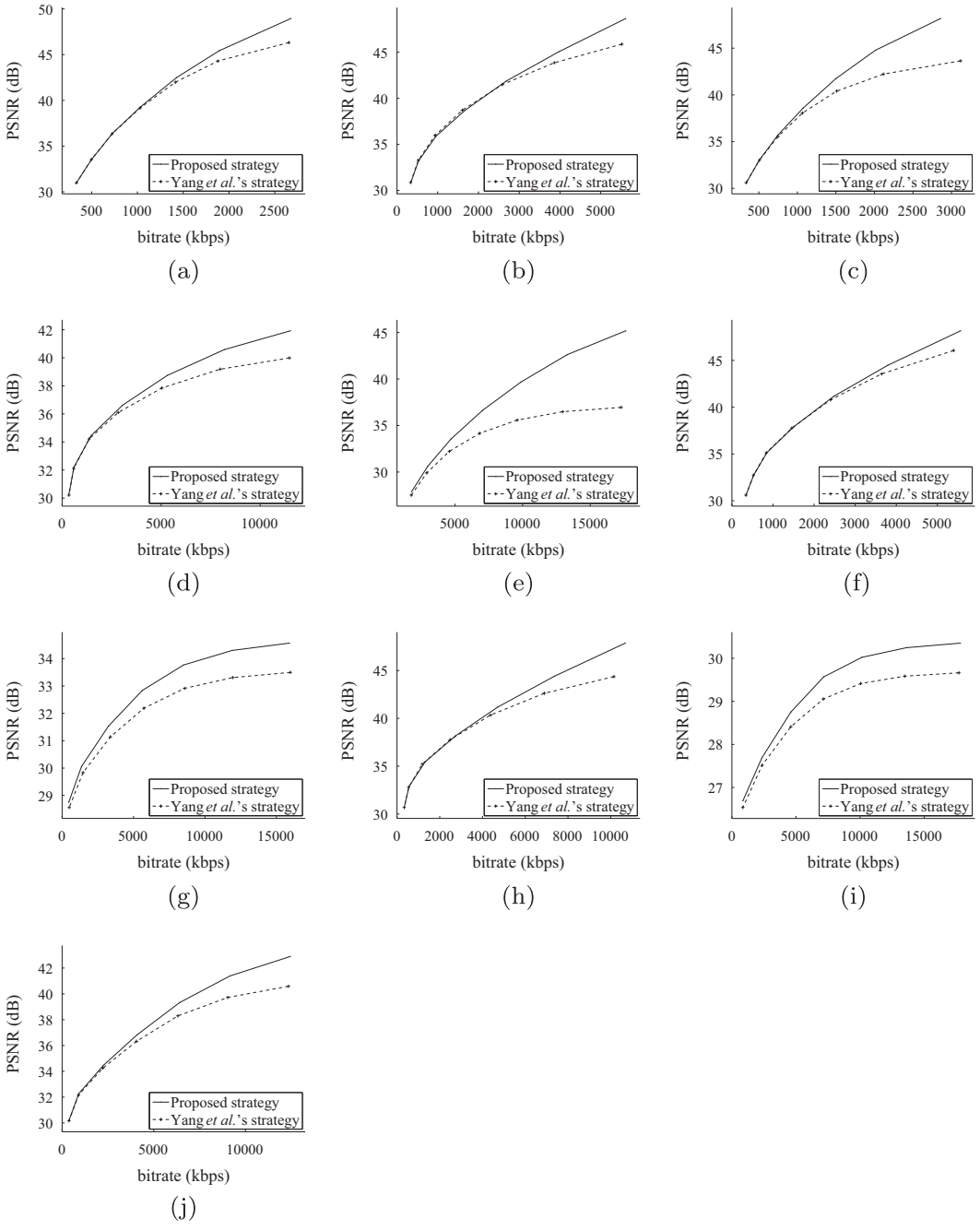

Fig. 6. RD curves of PSNR against bitrate corresponding to the two concerned subsampling strategies for the *Houses* video with different RGB CFA structures: (a) Bayer CFA. (b) Lukac and Plataniotis CFA. (c) Yamanaka CFA. (d) Diagonal stripe CFA. (e) Vertical stripe CFA. (f) Modified Bayer CFA. (g) HVS-based CFA. (h) Type I Pseudo-random CFA. (i) Type II Pseudo-random CFA. (j) Type III Pseudo-random CFA.

$\widehat{F}^C_M(i,j)$ in the above equation with $F^C_M(i,j)$ and rewrite the equation, and then the RGB color deviation-free Y component for the pixel at position (i,j) can be determined as follows

$$Y^*(i,j) = \begin{cases} \frac{F^C_M(i,j) - 1.596\times(V^*-128)}{1.164} + 16, & \text{if } C = R, \\ \frac{F^C_M(i,j) + 0.391\times(U^*-128) + 0.813\times(V^*-128)}{1.164} + 16, & \text{if } C = G, \\ \frac{F^C_M(i,j) - 2.018\times(U^*-128)}{1.164} + 16, & \text{if } C = B. \end{cases} \quad (6)$$

The same strategy is applied to the remaining three pixels of the current block for the determination of their RGB color deviation-free Y components.

When all the 2×2 blocks in the YUV images have been subsampled as described earlier, then the subsampled YUV images are conveyed to the H.264/AVC encoder for compression. Since Yang et al.'s chroma subsampling strategy only subsamples one pair of shared U and V components for one 2×2 YUV block, the information loss due to discarding three-quarters of U and V components leads to that the subsampled YUV block cannot be losslessly reversed into the original mosaic block prior to compression. When conveying such the subsampled YUV block with quality degradation for compression, accompanied by the compression distortion, the quality of the reconstructed mosaic video using Yang et al.'s subsampling strategy would decay more seriously. In contrast, the proposed improved subsampling strategy further modifies, given the shared U and V components, the Y components in the subsampled YUV block such that, prior to compression, the color values of the pixels in the reversed mosaic block corresponding to the current subsampled YUV block can be kept the same as those in the original mosaic block, i.e., solving the RGB color deviation

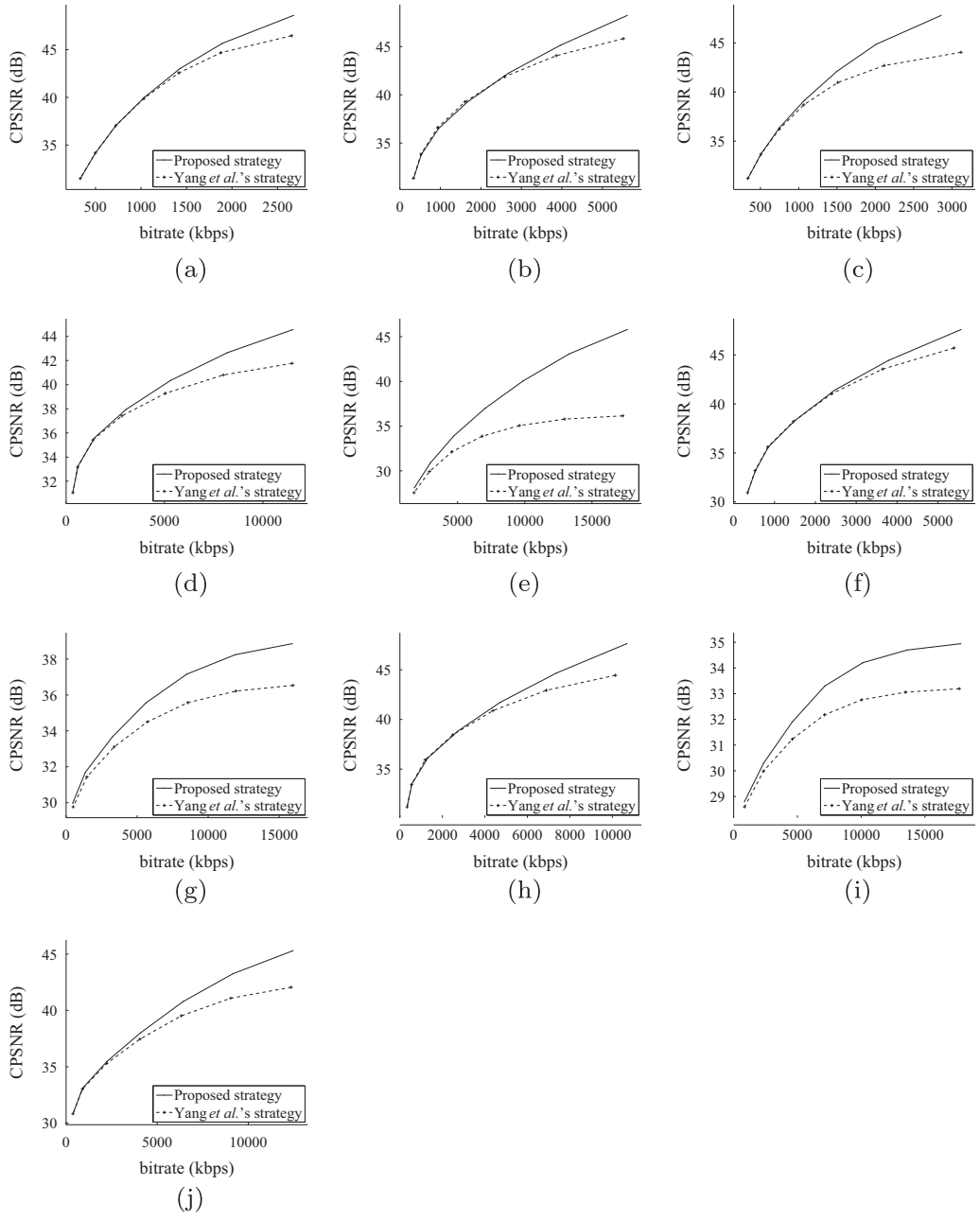

Fig. 7. RD curves of CPSNR against bitrate corresponding to the two concerned subsampling strategies for the *Houses* video with different RGB CFA structures: (a) Bayer CFA. (b) Lukac and Plataniotis CFA. (c) Yamanaka CFA. (d) Diagonal stripe CFA. (e) Vertical stripe CFA. (f) Modified Bayer CFA. (g) HVS-based CFA. (h) Type I Pseudo-random CFA. (i) Type II Pseudo-random CFA. (j) Type III Pseudo-random CFA.

problem. By conveying the subsampled YUV block without the RGB color deviations for compression, even though suffering from the compression distortion, the quality of the reconstructed mosaic video using the proposed improved subsampling strategy still can be expected to decay less than that using Yang et al.'s one.

3. Experimental results

We conducted several experiments to evaluate the performance of the proposed improved universal subsampling strategy for compressing mosaic videos with arbitrary RGB CFA structures in H.264/AVC. For comparison, the proposed subsampling strategy was compared with Yang et al.'s one. Four test videos, each with two hundred 352×288 image frames captured using three-sensor devices and normalized to 8-bit per channel RGB representation, were adopted from Kodak collection [13] and are shown in Fig. 5. Following the standard practice in [14,15,10,19], we first sampled each test video with the ten RGB CFA structures shown in Fig. 2 to obtain the mosaic videos. We then performed the compression and reconstruction processes with Yang et al.'s and the proposed subsampling strategies on these mosaic videos.

The H.264/AVC reference software JM 18.0 was adopted for video compression in the experiments. In addition, the size of the group of picture (GOP) was set to be 10, the GOP structure used was IPPP, and the seven different quantization parameters (QPs) considered in the compression process were 8, 12, 16, 20, 24, 28, and 32. The two concerned subsampling strategies and JM 18.2 were realized in Visual C++ 2008 and implemented on an IBM compatible computer with Intel i7-3770 CPU 3.4 GHz, 16 GB RAM, and Microsoft Windows 7 64-bit operating system. Furthermore, all the compression results can be found in [20].

3.1. Performance evaluation metrics

The quality of the reconstructed mosaic video and the storage requirement in terms of peak signal-to-noise ratio (PSNR) and bitrate, respectively, were the main performance measures for comparison. In addition, since the mosaic videos eventually needs to be recovered to the full-color videos for display purposes, the original mosaic videos and the reconstructed ones were demosaicked to full-color videos using the universal demosaicking technique modified from [15] and the color PSNR (CPSNR) was

Table 1
BD-PSNR (in dB) of the proposed subsampling strategy over Yang et al.'s one for the four test videos with the ten RGB CFA structures.

CFA structure	Test video	BD-PSNR	
		Reconstructed mosaic video	Reconstructed full-color video
Bayer CFA	Houses	0.443	0.369
	Lighthouse	0.200	0.141
	Nature	0.307	0.254
	Wall	0.291	0.255
Lukac and Plataniotis CFA	Houses	0.208	0.175
	Lighthouse	0.122	0.083
	Nature	0.091	0.074
	Wall	0.245	0.220
Yamanaka CFA	Houses	1.071	0.900
	Lighthouse	0.537	0.414
	Nature	0.404	0.330
	Wall	0.407	0.305
Diagonal stripe CFA	Houses	0.395	0.502
	Lighthouse	0.219	0.240
	Nature	0.565	0.680
	Wall	0.323	0.351
Vertical stripe CFA	Houses	2.467	3.078
	Lighthouse	1.948	2.606
	Nature	1.792	1.884
	Wall	1.421	1.771
Modified Bayer CFA	Houses	0.216	0.202
	Lighthouse	0.053	0.037
	Nature	0.405	0.393
	Wall	0.172	0.160
HVS-based CFA	Houses	0.489	0.779
	Lighthouse	0.645	0.880
	Nature	0.643	0.959
	Wall	0.557	0.817
Type I Pseudo-random CFA	Houses	0.348	0.313
	Lighthouse	0.166	0.137
	Nature	0.417	0.367
	Wall	0.254	0.234
Type II Pseudo-random CFA	Houses	0.329	0.666
	Lighthouse	0.237	0.478
	Nature	0.193	0.545
	Wall	0.075	0.246
Type III Pseudo-random CFA	Houses	0.483	0.624
	Lighthouse	0.367	0.413
	Nature	0.548	0.661
	Wall	0.415	0.477
Average		0.520	0.601

calculated between them as another quality measure. Denote by $\mathbb{P} = \{(m,n)|1 \leqslant m \leqslant H, 1 \leqslant n \leqslant W\}$ the set of pixel coordinates in one image frame of size $W \times H$. The PSNR of a reconstructed mosaic video with N image frames of size $W \times H$ can be expressed as

$$\mathrm{PSNR} = 10\log_{10}\frac{255^2}{\frac{1}{NWH}\sum_{n=1}^{N}\sum_{p\in\mathbb{P}}\left[I_M^n(p) - \widetilde{I}_M^n(p)\right]^2}, \tag{7}$$

where $I_M^n(p)$ denotes the color value of the pixel at position p in the n-th mosaic image frame of the original mosaic video and $\widetilde{I}_M^n(p)$ represents the reconstructed analog. The CPSNR of a reconstructed full-color video can be expressed as

$$\mathrm{CPSNR} = 10\log_{10} \times \frac{255^2}{\frac{1}{3NWH}\sum_{n=1}^{N}\sum_{p\in\mathbb{P}}\sum_{C\in\{R,G,B\}}\left[I_{RGB}^{n,C}(p) - \widetilde{I}_{RGB}^{n,C}(p)\right]^2}, \tag{8}$$

where $I_{RGB}^{n,C}(p)$ and $\widetilde{I}_{RGB}^{n,C}(p)$ denote the $C \in \{R,G,B\}$ color value of the pixel at position p in the n-th image frame of the original and reconstructed full-color videos, respectively. In general, higher values of PSNR and CPSNR indicate better quality of the reconstructed mosaic video and the reconstructed full-color video, respectively, while lower bitrate values imply less storage requirement.

3.2. Performance comparison of the subsampling strategies

Rate-distortion (RD) curves, which depict the PSNR against bitrate or the CPSNR against bitrate with different QPs, for the two concerned subsampling strategies based on the *Houses* test video with the ten RGB CFA structures were plotted in Figs. 6 and 7, respectively. Due to lack of space, the similar RD curves for the two concerned subsampling strategies based on the other three test videos with the ten RGB CFA structures can be found in [20]. The results of the four test videos with the ten RGB CFA structures showed that with respect to the quality of the reconstructed mosaic and full-color videos under the same bitrate, the proposed subsampling strategy outperformed Yang et al.'s one in the low and middle QP situations. Although the proposed subsampling strategy was competitive with Yang et al.'s one in the high QP situation, it seldom occurs in practice since a low bitrate coding often leads to serious quality degradation and visual discomfort in the reconstructed full-color videos.

Furthermore, taking Yang et al.'s subsampling strategy as the comparison basis, Bjøntegaard delta PSNR (BD-PSNR) [2], which measures the average difference in PSNR and CPSNR between two RD curves, for the proposed subsampling strategy was calculated over QP = 8, 16, 24, and 32 to provide quantitative comparison results. Here, the calculation of BD-PSNR follows the three steps: (1) select four points from each of the two compared RD curves, which are often the results corresponding to the four concerned QPs, and then fit each curve with a third-order polynomial by the selected four points, (2) compute the integral over an interval of bitrate for each fitted curve, and (3) BD-PSNR is calculated as the difference between the two integrals divided by the bitrate interval. The values of BD-PSNR corresponding to the proposed subsampling strategy for the four test videos with the ten RGB CFA structures were given in Table 1, and the positive values of BD-PSNR indicate the quality superiority of our proposed subsampling strategy for compressing mosaic videos with arbitrary RGB CFA structures in H.264/AVC with the same bitrate. The results in Table 1 showed that the average BD-PSNRs of the proposed subsampling strategy over Yang et al.'s were, respectively, 0.520 dB and 0.601 dB, indicating clear improvement in the quality of the reconstructed mosaic videos and the reconstructed full-color videos.

Besides the objective metrics, the subjective visual evaluation was used to demonstrate the quality superiority of the proposed improved subsampling strategy over Yang et al.'s one. In general, mosaic videos are not directly used for display, so only the reconstructed full-color videos using the two concerned subsampling

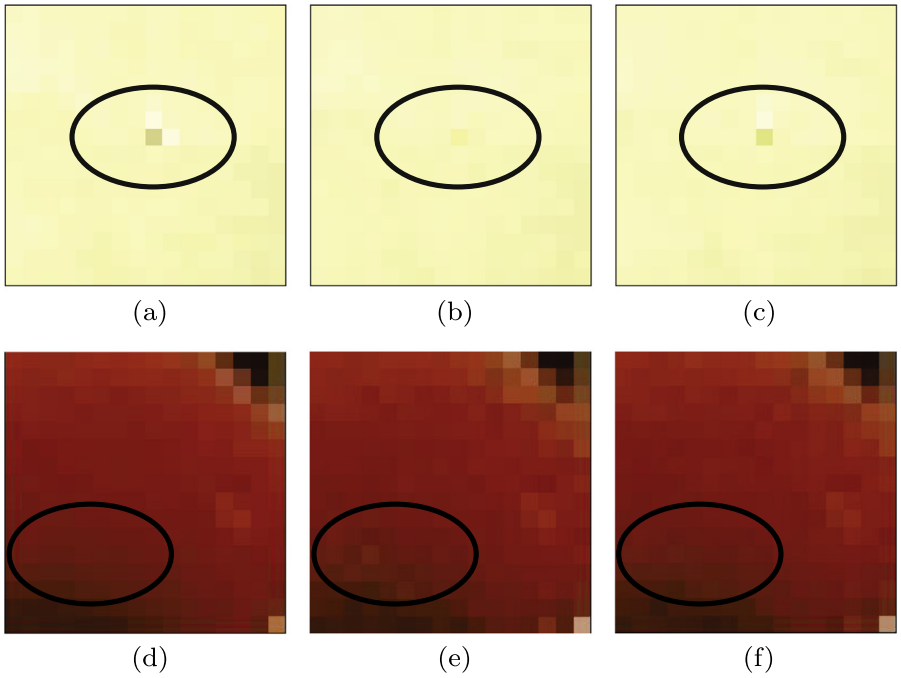

Fig. 8. Subjective visual evaluation on the *Houses* and *Lighthouse* test videos: (a)–(c) magnified subimages cut from the original demosaicked *Houses* video, the reconstructed full-color *Houses* video generated by Yang et al.'s subsampling strategy, and the reconstructed full-color *Houses* video generated by the proposed subsampling strategy; (d)–(f) magnified subimages cut from the original demosaicked *Lighthouse* video, the reconstructed full-color *Lighthouse* video generated by Yang et al.'s subsampling strategy, and the reconstructed full-color *Lighthouse* video generated by the proposed subsampling strategy.

Table 2
The subsampling time and the average compression time (in second) for Yang et al.'s and the proposed subsampling strategies.

CFA structure	Test video	Subsampling time		Average compression time	
		Yang et al.'s	Proposed	Yang et al.'s	Proposed
Bayer CFA	Houses	1.50	1.95	791.36	793.26
	Lighthouse	1.45	1.97	764.70	759.50
	Nature	1.51	1.90	834.44	838.29
	Wall	1.48	1.90	791.55	793.79
Lukac and Plataniotis CFA	Houses	1.45	1.89	820.84	821.10
	Lighthouse	1.48	1.90	772.35	777.66
	Nature	1.50	1.93	911.40	929.66
	Wall	1.45	1.97	795.23	810.37
Yamanaka CFA	Houses	1.47	1.98	805.62	805.86
	Lighthouse	1.45	1.94	793.63	788.92
	Nature	1.47	1.92	846.39	846.53
	Wall	1.45	1.92	817.56	827.01
Diagonal stripe CFA	Houses	1.50	1.90	857.77	863.50
	Lighthouse	1.45	1.90	829.01	840.35
	Nature	1.45	1.93	899.87	918.69
	Wall	1.48	1.92	751.05	759.67
Vertical stripe CFA	Houses	1.45	1.90	949.39	942.14
	Lighthouse	1.45	1.90	823.00	821.69
	Nature	1.47	1.90	888.95	888.54
	Wall	1.45	1.90	873.24	873.19
Modified Bayer CFA	Houses	1.54	1.92	816.00	823.08
	Lighthouse	1.50	1.90	791.98	807.33
	Nature	1.44	1.90	847.95	858.78
	Wall	1.48	1.90	694.98	710.46
HVS-based CFA	Houses	1.45	1.92	914.84	908.36
	Lighthouse	1.47	1.97	860.61	858.15
	Nature	1.45	1.94	949.56	944.06
	Wall	1.44	1.93	887.79	891.08
Type I Pseudo-random CFA	Houses	1.50	1.93	861.36	864.02
	Lighthouse	1.47	1.94	818.10	825.38
	Nature	1.50	2.00	785.07	789.94
	Wall	1.48	2.01	707.69	724.69
Type II Pseudo-random CFA	Houses	1.45	1.94	924.88	922.27
	Lighthouse	1.45	1.94	864.12	862.63
	Nature	1.47	1.92	954.19	958.10
	Wall	1.45	1.93	891.86	896.45
Type III Pseudo-random CFA	Houses	1.47	1.93	882.87	884.96
	Lighthouse	1.53	1.92	823.52	838.87
	Nature	1.48	1.94	777.96	798.11
	Wall	1.47	1.93	735.41	750.66
Average		1.47	1.93	835.20	840.42

strategies were adopted for visual comparison. Fig. 8(a)–(c) showed the magnified subimages from the original demosaicked *Houses* video and from the reconstructed full-color *Houses* videos generated, respectively, by the two concerned subsampling strategies with QP = 8, while Fig. 8(d)–(f) showed the analog from the *Lighthouse* video. From the regions circled by the black lines in Fig. 8(a)–(f), it was clear that the reconstructed full-color subimages by the proposed subsampling strategy demonstrated less RGB color deviations in comparison with those by Yang et al.'s one, leading to a better visual perception.

3.3. Computational complexity comparison

To demonstrate the feasibility of a subsampling strategy, the evaluation on computational complexity should be addressed. This subsection investigated the computational time complexity for comparison of the proposed subsampling strategy with Yang et al.'s one. Specifically, we measured the computational time spent in the subsampling for each concerned subsampling strategy and each test video with the ten RGB–CFA structures. In addition, since the Y components are modified in the proposed subsampling strategy but not in Yang et al.'s one, which may affect the required time for the subsequent encoding, we also measured the average computational time spent in the whole compression procedure over the seven considered QPs for each concerned subsampling strategy and each test video with the ten RGB–CFA structures.

Table 2 summarized the related subsampling time and compression time of the two concerned subsampling strategies. As displayed in Table 2, although the proposed subsampling strategy increased the subsmpling time by $(1.93 - 1.47)/1.47 = 31.29\%$ on average, it only caused a slight increase about $(840.42 - 835.20)/835.20 = 0.62\%$ in the average compression time, implying that compression of mosaic videos using the proposed subsampling strategy is competitive in terms of computational complexity with Yang et al.'s one. Furthermore, the average computational time required for compressing a mosaic image frame by the proposed subsampling strategy was only $(840.42\ \text{s}/200\ \text{frames}) = 4.20\ \text{s}$, indicating that compression of mosaic videos using the proposed subsampling strategy is feasible in practice.

4. Conclusion

We have presented the proposed improved universal subsampling strategy for compressing mosaic videos with arbitrary RGB

CFA structures in H.264/AVC. Under the framework of Yang et al.'s universal subsampling strategy, we replace retaining the original Y luma component with adopting a novel modification for the Y luma component such that the RGB color deviation problem can be resolved prior to compression, leading to better quality of the reconstructed mosaic video and the reconstructed full-color video. The experimental results of the four test videos with the ten commonly used RGB CFA structures demonstrated that the proposed improved universal subsampling strategy achieves better quality of the reconstructed mosaic videos and the reconstructed full-color videos under the same bitrate when compared with the state-of-the-art one by Yang et al. Furthermore, it would be interesting to extend the results of this work to deal with the digital time delay integration images [3], in which each pixel has two RGB primary color components.

Acknowledgments

This work was supported by the National Science Council of Taiwan, under the Contracts NSC101-2221-E-011-139-MY3 and NSC102-2221-E-011-055-MY3.

References

[1] B.E. Bayer, Color Imaging Array, U.S. Patent No. 3971065, 1976.
[2] G. Bjontegaard, Calculation of average PSNR differences between RD curves, in: VECG-M33, ITU-T VECG Meeting, Austin, Texas, 2001, pp. 2–4.
[3] E. Bodenstorfer, J. Fürtler, J. Brodersen, K.J. Mayer, C. Eckel, K. Gravogel, H. Nachtnebel, High speed line-scan camera with digital time delay integration, in: Proc. of SPIE 6496, Real-Time Image Processing, 2007, pp. 1–10.
[4] H. Chen, M. Sun, E. Steinbach, Compression of Bayer-pattern video sequences using adjusted chroma subsampling, IEEE Trans. Circ. Syst. Video Technol. 19 (12) (2009) 1891–1896.
[5] Draft ITU-T Recommendation and Final Draft International Standard of Joint Video Specification, document ITU-T Rec. H.264/ISO/IEC 14 496-10 AVC, Joint Video Team of ISO/IEC and ITU-T, 2003.
[6] C. Doutre, P. Nasiopoulos, K.N. Plataniotis, H.264-based compression of Bayer pattern video sequences, IEEE Trans. Circ. Syst. Video Technol. 18 (6) (2008) 725–734.
[7] C. Doutre, P. Nasiopoulos, Modified H.264 intra prediction for compression of video and images captured with a color filter array, in: Proc. of IEEE International Conference on Image Processing, 2009, pp. 3401–3404.
[8] S. Farsiu, M. Elad, P. Milanfar, Multiframe demosaicing and super-resolution of color images, IEEE Trans. Image Process. 15 (1) (2006) 141–159.
[9] F. Gastaldi, C.C. Koh, M. Carli, A. Neri, S.K. Mitra, Compression of videos captured via Bayer patterned color filter arrays, in: Proc. of 13th European Signal Processing Conference, 2005, pp. 983–992.
[10] B.K. Gunturk, J. Glotzbach, Y. Altunbasak, R.W. Schaffer, R.M. Murserau, Demosaicking: color filter array interpolation, IEEE Signal Process. Mag. 22 (1) (2005) 44–54.
[11] D. Heiss-Czedik, R. Huber-Mörk, D. Soukup, H. Penz, B.L. García, Demosaicing algorithms for area- and line-scan cameras in print inspection, J. Vis. Image Commun. Represent. 20 (6) (2009) 389–398.
[12] B.K. Karch, R.C. Hardie, Adaptive wiener filter super-resolution of color filter array images, Opt. Express 21 (16) (2013) 18820–18841.
[13] Kodak True Color Image Collection. <http://r0k.us/graphics/kodak/>.
[14] R. Lukac, K. Martin, K.N. Plataniotis, Digital camera zooming based on unified CFA image processing steps, IEEE Trans. Consum. Electron. 50 (1) (2004) 15–24.
[15] R. Lukac, K.N. Plataniotis, Universal demosaicking for imaging pipelines with an RGB color filter array, Pattern Recogn. 38 (11) (2005) 2208–2212.
[16] R. Lukac, K.N. Plataniotis, Color filter arrays: design and performance analysis, IEEE Trans. Consum. Electron. 51 (4) (2005) 1260–1267.
[17] J. Nakamura, Image Sensors and Signal Processing for Digital Still Cameras, CRC, Boca Raton, FL, 2005.
[18] S.C. Pei, I.K. Tam, Effective color interpolation in CCD color filter arrays using signal correlation, IEEE Trans. Circ. Syst. Video Technol. 13 (6) (2003) 503–513.
[19] W.J. Yang, K.L. Chung, W.N. Yang, L.C. Lin, Universal chroma subsampling strategy for compressing mosaic video sequences with arbitrary RGB color filter arrays in H.264/AVC, IEEE Trans. Circ. Syst. Video Technol. 23 (4) (2013) 591–606.
[20] http://140.118.175.164/YHChiu/paper/UniversalSubsampling/.